Investigation of inhibition effect of daidzein on osteosarcoma cells based on experimental validation and systematic pharmacology analysis

Yufan Zhu [1] , **Zhiqiang Yang** [1] , **Yuanlong Xie** [1] , **Min Yang** [1] , **Yufeng Zhang** [1] , **Zhouming Deng** [Corresp., 1] , **Lin Cai** [Corresp. 1]

[1] Department of Spine Surgery & Musculoskeletal Tumor, Zhongnan Hospital of Wuhan University, Wuhan, Hubei, People's Republic of China

Corresponding Authors: Zhouming Deng, Lin Cai
Email address: dengzhouming@whu.edu.cn, orthopedics@whu.edu.cn

Objective: This study aims to explore the effect of daidzein, which is a natural isoflavone compound mainly extracted from soybeans, on osteosarcoma and the potential molecular mechanism.

Material and methods: 143B and U2OS osteosarcoma cells were treated with gradient concentrations of daidzein, and MTT assay was used to determine the cell proliferation capacity and $IC_{50.}$ Hoechst 33342 staining and Annexin V-FITC/PI detection were used to determine apoptosis. Cell cycle was analyzed by flow cytometry, and migration ability were detected by transwell assays and scratch wound assay. An osteosarcoma xenograft mice model was applied to investigate the effect of daidzein on osteosarcoma in vivo. Systematic pharmacology and molecular modeling analysis were applied to predict the target of daidzein to osteosarcoma, and the target Src was verified by western blotting. We also observed the effect of daidzein on cell proliferation and apoptosis of Src-overexpressing osteosarcoma cells.

Results: In vitro, daidzein significantly inhibited 143B and U2OS osteosarcoma cell proliferation and migration, and induced cell cycle arrest. In vivo, Daidzein exerts antitumor effects in osteosarcoma xenograft mice. After systematic screening and analysis, Src-MAPK signaling pathway was predicted as the highest-ranked pathway. Western blot demonstrated that daidzein inhibited phosphorylation of the Src-ERK pathway in osteosarcoma cells. And overexpression of Src could partially reverse the inhibitory effects of daidzein on osteosarcoma cell proliferation.

Conclusion: Daidzein exerts an antitumor effect on osteosarcoma, the mechanism may be through the Src-ERK pathway.

1 # Investigation of inhibition effect of daidzein on
2 # osteosarcoma cells based on experimental validation
3 # and systematic pharmacology analysis

5 Yufan Zhu[1], Zhiqiang Yang[1], Yuanlong Xie[1], Min Yang[1], Yufeng Zhang[1], Zhouming Deng[1], Lin
6 Cai[1]

8 [1] Department of Spine Surgery & Musculoskeletal Tumor, Zhongnan Hospital of Wuhan
9 University, Wuhan, Hubei, PR China

11 Corresponding Author:
12 Lin Cai[1]
13 #169, East Lake Road, Wuchang District, Wuhan, Hubei, 430072, PR China
14 Email address: orthopedics@whu.edu.cn
15 Zhouming Deng[1]
16 #169, East Lake Road, Wuchang District, Wuhan, Hubei, 430072, PR China
17 Email address: dengzhouming@whu.edu.cn

19 ## Abstract

20 **Objective:** This study aims to explore the effect of daidzein, which is a natural isoflavone
21 compound mainly extracted from soybeans, on osteosarcoma and the potential molecular
22 mechanism.
23 **Material and methods:** 143B and U2OS osteosarcoma cells were treated with gradient
24 concentrations of daidzein, and MTT assay was used to determine the cell proliferation capacity
25 and IC_{50}. Hoechst 33342 staining and Annexin V-FITC/PI detection were used to determine
26 apoptosis. Cell cycle was analyzed by flow cytometry, and migration ability were detected by
27 transwell assays and scratch wound assay. An osteosarcoma xenograft mice model was applied
28 to investigate the effect of daidzein on osteosarcoma in vivo. Systematic pharmacology and
29 molecular modeling analysis were applied to predict the target of daidzein to osteosarcoma, and
30 the target Src was verified by western blotting. We also observed the effect of daidzein on cell
31 proliferation and apoptosis of Src-overexpressing osteosarcoma cells.
32 **Results:** In vitro, daidzein significantly inhibited 143B and U2OS osteosarcoma cell
33 proliferation and migration, and induced cell cycle arrest. In vivo, Daidzein exerts antitumor
34 effects in osteosarcoma xenograft mice. After systematic screening and analysis, Src-MAPK
35 signaling pathway was predicted as the highest-ranked pathway. Western blot demonstrated that
36 daidzein inhibited phosphorylation of the Src-ERK pathway in osteosarcoma cells. And
37 overexpression of Src could partially reverse the inhibitory effects of daidzein on osteosarcoma
38 cell proliferation.

39 **Conclusion:** Daidzein exerts an antitumor effect on osteosarcoma, the mechanism may be
40 through the Src-ERK pathway.

Introduction

42 Osteosarcoma is the most common primary tumor of bone in children and adolescent. The 5-year
43 survival rate of patients with localized osteosarcoma is approximately 70%, whereas the overall
44 survival rate of patients with metastatic or recurrent disease is less than 20% (Harrison et al.
45 2018). Based on historical data, over 80% of patients will develop metastasis following resection
46 of the primary tumor alone, and even with the addition of chemotherapy to primary tumor
47 resection, approximately one-third of patients presenting with localized disease will subsequently
48 develop pulmonary metastases (Khanna et al. 2014). Standard treatment modalities consist of
49 combining surgical excision with chemotherapy, which has changed very little over the past 30
50 years (Gianferante et al. 2017; Li et al. 2020; Luu & Viloria-Petit 2020). The three-drug
51 chemotherapy regimen of cisplatin, doxorubicin, and methotrexate (MAP) forms the backbone
52 therapy, and the response to induction chemotherapy correlates with patient outcome
53 (Kleinerman 2016). Due to the clinical heterogeneity of osteosarcoma, the selection of treatment
54 options and effective drug combinations remain limited. It is generally accepted that plants are
55 regarded as valuable resources for the development of drugs to treat many diseases, including
56 cancer (Thomford et al. 2018). Some natural active ingredients display strong antitumor activity;
57 in addition, compared with chemotherapy, they have fewer adverse effects and no resistance to
58 chemotherapy. Therefore, there is an urgent requirement to examine novel and more effective
59 natural compounds for the treatment of osteosarcoma.
60 Flavonoids are phenolic compounds with more than 6000 family members that widely exist in a
61 large number of plants and fungi. Isoflavone is a natural flavonoid that plays the role of
62 phytoestrogens in mammals and has become a research hotspot in recent years (Zhang et al.
63 2018). Daidzein, whose chemical composition is 7,4-dihydroxyisoflavone, belongs to the
64 isoflavone family. It is the most frequently ingested and deeply studied phytoestrogen (Jin et al.
65 2010). In previous studies, daidzein has been proven to have antitumor effects on a variety of
66 tumors, including breast cancer (Bao et al. 2014; Magee et al. 2014), bladder cancer (He et al.
67 2016), prostate cancer (Singh-Gupta et al. 2010; Yu et al. 2003), colon cancer (Liang et al.
68 2018), endometrial carcinogenesis (Lian et al. 2001), melanoma (Wang et al. 2002),
69 neuroblastoma (Lo et al. 2007), and choriocarcinoma (Zheng et al. 2017). Recently, Luisa
70 Salvatori et al. reported that daidzein inhibited proliferation and cell cycle progression and
71 promoted apoptosis in a U2OS human osteosarcoma cell line in vitro (Salvatori et al. 2009), but
72 there has been no research on the related mechanism. In addition, no other study has
73 demonstrated that daidzein is capable of inhibiting osteosarcoma. Therefore, we carried out an
74 in-depth study on the effect and mechanisms of daidzein against osteosarcoma.
75 Systemic pharmacology, proposed by Andrew L. Hopkins, is an emerging discipline that
76 integrates systems biology and pharmacology (Hopkins 2008). It provides a new way to explore
77 the mechanism of drugs from the molecular and cellular levels to the tissue and organism levels
78 (Berger & Iyengar 2009). After verifying the inhibitory effects of daidzein on osteosarcoma in

79 vitro and in vivo, we applied systemic pharmacology theory and molecular docking analysis to
80 identify the intersection of potential targets between osteosarcoma and daidzein, and selected the
81 key target, Src, and its downstream MAPK pathway. Finally, a rescue experiment was carried
82 out to validate the mechanisms of action. The methodological flowchart of this study is shown in
83 Figure 1.

Materials & Methods

1. Reagents

Daidzein [7-hydroxy-3- (4-hydroxyphenyl) chromen-4-one] was purchased from Aladdin
Industrial, Inc. (Shanghai, China), which with a purity over 98%. It was dissolved in DMSO at a
final concentration of 100 mM in medium and stored at -20°C. Dimethyl sulfoxide (DMSO) was
obtained from Sinopharm Chemical Reagent Co., Ltd. (China).

2. Cell culture

Human osteosarcoma cell lines (143B and U2OS) and human osteoblast cell line hFOB 1.19
were obtained from the China Centre for Type Culture Collection (Wuhan, China). 143B cells
were cultured in Roswell Park Memorial Institute (RPMI) 1640 medium supplemented with 10%
heat - inactivated FBS (Gibco) and 1% antibiotics in a 37°C incubator with 5% CO_2. U2OS cells
were cultured in McCoy's 5A medium (modified) when hFOB 1.19 was cultured in α-MEM
(HyClone) and the other conditions were the same as those used for 143B cells.

3. Cell proliferation analysis

Cells were plated in 96-well plates at a density of 2000 cells per well and incubated at 37°C for
12 h. Then, the cells were treated for the indicated time periods with different concentrations of
daidzein diluted in medium containing 10% FBS. After incubation, the supernatants were
removed, and MTT solution (Beyotime, Shanghai, China) was added to each well (100 μL per
well). Following incubation at 37°C in a dark environment for an additional 4 h, the supernatants
were removed again, and 200 μL DMSO was added to each well to solubilize formazan. After 10
min, the 96-well plates were placed in a microplate reader, and the absorbance was recorded at
570 nm. The data came from three independent experiments, each with six copies. The mean cell
viability of the treated cells was used to calculate the survival fractions.

4. Colony formation assay

The cells were evenly seeded in a 6-well plate at a density of 500 cells per well. After 24 h, the
cells were treated with different concentrations of daidzein for approximately 7 days until the
cells grew into visible colonies. Then, the supernatant was discarded, and the cells were washed
with PBS three times. Colonies were then fixed with 4% paraformaldehyde for 30 min and
stained with 1% crystal violet for 10 min. The number of colonies (more than 50 cells/colony)
was counted and quantified.

5. Cell apoptosis and cycle detection

Following exposure to daidzein for a specified period, osteosarcoma cells were collected for
apoptosis and cycle detection. Hoechst 33342 (Beyotime, Shanghai, China) was used to detect
cell apoptosis by observing the cell morphology. After osteosarcoma cells were treated, the
medium was discarded, and the cells were washed twice with PBS and then fixed with sufficient

119 4% paraformaldehyde at 4°C for 10 min. Then, sufficient Hoechst 33342 staining solution was
120 added to cover the cells. After incubation in the dark for 10 min, the cells were washed with PBS
121 and then immediately observed and imaged by fluorescence microscopy. In addition, cell
122 apoptosis and cell cycle progression were analyzed by flow cytometry. Cell apoptosis of human
123 osteosarcoma cells was analyzed based on Annexin V-FITC/propidium iodide (PI) dual staining
124 when the cell cycle was assessed by staining cells with 20 μg/mL PI.

125 **6. Migration ability detection**
126 The migration ability of osteosarcoma cells was detected by Transwell migration assay and
127 scratch wound assay. The Transwell experimental procedure was as follows: Approximately
128 5×10^4 cells suspended in 100 μL serum-free RPMI 1640 or McCoy's 5A medium were added to
129 each upper chamber, and 600 μL of medium containing 10% FBS was added to the lower
130 chamber. Cells were cultured at 37°C for 24 h, fixed with 4% paraformaldehyde for 30 min and
131 stained with 1% crystal violet for 10 min. Cotton swabs were used to remove the unmigrated
132 cells on the upper surface of the membrane, and the cells that migrated on the lower surface of
133 the film were counted. As for scratch wound assays, cells were plated in a 6-well plate at a
134 density of 5×10^5 cells per well and then incubated at 37°C until almost complete confluence.
135 Three parallel wounds were made with a 10 μL pipette tip per well. Cells were cultured in
136 serum-free medium supplemented with different concentrations of daidzein. At 0h and 24h,
137 photos were taken at the same position under an optical microscope, and the wound width of
138 each group was compared.

139 **7. Establishment of a nude mouse osteosarcoma xenograft model**
140 Twelve four-week-old male BALB/c nude mice obtained from Hubei Experimental Animal
141 Research Center (Hubei, China) were used for animal experiments. 143B cells were digested and
142 suspended in cold PBS at a final concentration of 1×10^7 cells per mL. In this model, a total of
143 100μL of the prepared cell suspension was injected in the right subaxillary area subcutaneously.
144 7 days after tumor inoculation, when the volume of the tumor was approximately 100 mm^3,
145 daidzein (20 mg/kg) was administered by tail vein injection every 2 days in the experimental
146 group (n=6), while the control group (n=6) was injected with an equal volume of DMSO. The
147 injection treatment lasted for 9 days, and the tumor volume and mouse body weight were
148 measured every 3 days. Tumor volume (mm^3) was calculated using the following equation:
149 length×width^2×0.5. On day 16, mice were sacrificed by dislocation of cervical vertebra after
150 anesthesia with sodium pentobarbital (100mg/kg body weight, tail vein injection), and the
151 xenografts were dissected and fixed with 4% polyformaldehyde for H&E staining analysis.
152 When the tumor diameter exceeded 20mm or rupture and infection occurred, as well as when
153 treatment was ineffective after systemic infection occurred, mice were euthanized using the
154 method described above.
155 This in vivo study was conducted according to the guidelines of the Declaration of Helsinki, and
156 approved by the Institutional Review Board (or Ethics Committee) of Institutional Animal Care
157 and Use Committee, Wuhan University Center for Animal Experiment (protocol code WP2020-
158 08106. On August 10th, 2020).

159 **8. Target identification and network construction**
160 The osteosarcoma-related targets were collected and combined from the following databases:
161 DigSeE (http://210.107.182.61/geneSearch/), DisGeNET (http://www.disgenet.org/), GeneCards
162 (https://www.genecards.org/), KEGG disease (https://www.kegg.jp/kegg/disease/), MalaCards
163 (http://www.malacards.org/), and Phenopedia
164 (https://phgkb.cdc.gov/PHGKB/startPagePhenoPedia.action). The validated targets of daidzein
165 were extracted from PubChem (https://pubchem.ncbi.nlm.nih.gov/) and PharmMapper
166 (http://www.lilabecust.cn/pharmmapper/). Common targets of osteosarcoma and daidzein were
167 discovered and retained by VENNY 2.1.0 (https://bioinfogp.cnb.csic.es/tools/venny/) for further
168 analysis. A protein-protein interaction (PPI) network was constructed by STRING (https://string-
169 db.org/) and visualized by Cytoscape software. The Database for Annotation, Visualization and
170 Integrated Discovery (DAVID; http://david.abcc.ncifcrf.gov/) was used to perform GO and
171 pathway enrichment analyses, and Cytoscape software (Version 3.8.1) was used to construct the
172 target-function network.
173 **9. Molecular docking studies**
174 To identify the potential interaction between Src and daidzein, molecular docking simulations
175 were conducted with AutoDock Vina (version 1.1.2) to predict their preferred binding
176 conformation. PubChem was referenced for the SDF file of daidzein, and the SDF file was
177 transformed into a PDB file by Open Babel 2.3.2. The crystal structure of human Src was
178 derived from the Protein Data Bank (PDB) database (http://www.rcsb.org, PDB code: 2H8H).
179 Before molecular docking analysis, PYMOL 2.3.4 software was used to remove the water
180 molecules as well as ligands from the receptor protein, and AutodockTools software was used to
181 balance the charge and affix hydrogen atoms to the receptor protein. Grid Option was used to
182 adjust the number of grid points in each direction, the center of the binding pocket and the
183 spacing between the grid points. The centroid of the daidzein molecule in the crystal structures of
184 the complex was defined as the binding site. AutoDock Vina software was used for molecular
185 docking of the Src protein and daidzein molecule, and the results were output in the form of
186 affinity. The affinity is obtained by calculating the space effect, repulsion, hydrogen bond,
187 hydrophobic interaction and molecular flexibility of the complex, which is an important indicator
188 to measure whether the ligand can effectively bind to the receptor molecule. The lower the value,
189 the better the binding effect.
190 **10. Analysis of proteins in osteosarcoma cells treated with daidzein**
191 Cold PBS was used to wash the adherent osteosarcoma cells cultured in 6-well plates three times.
192 RIPA buffer containing a proteinase inhibitor (Beyotime, Shanghai, China) was used to extract
193 total protein from osteosarcoma cells. Osteosarcoma cells were scraped with a cell scraper,
194 dissolved in buffer, and transferred to a 1.5 mL EP tube with a pipette. The above samples were
195 treated with an ultrasonic cell breaker, with ultrasonic treatment for 3s and an interval time of
196 10s, which was repeated three times. Then, the lysates were centrifuged at 4°C and 13000 g for
197 15 min. In this way, the protein composition was separated and diluted for denaturation. Protein
198 samples were subjected to SDS-PAGE and then transferred to PVDF membranes. The blocking

199   solution was prepared by dissolving 5% skim milk powder in TBST, and the membrane was put
200   into the solution and blocked for 1h. The membranes were then incubated with the following
201   rabbit anti-human polyclonal primary antibodies overnight: anti-Src (ab109381), anti-p-Src
202   (ab40660, phospho Y418), anti-JNK (ab179461), anti-p-JNK (ab76572, phospho
203   Y185+Y185+Y223), anti-ERK (ab184699), anti-p-ERK (ab201015, phospho T202+T185), anti-
204   p38 (ab178867, phospho T180), anti-p-p38 (ab195049, phospho T180+Y182) and anti-GAPDH
205   (ab9485) (Abcam, Shanghai, China). GAPDH expression was used as a loading control. After
206   washing three times, the membranes were incubated with the corresponding goat anti-rabbit
207   secondary antibodies (Abcam, Shanghai, China). A Western blot visualization (ECL kit, Pierce,
208   USA) and analysis system (Bio-Rad) was used to detect chemiluminescence.

209   **11. Construction of Src-overexpressing osteosarcoma cell lines by lentivirus transfection**
210   For Src overexpression, 143B and U2OS cells were transfected with 4 µg of pMSCV-Flag or
211   pMSCV-Flag-Src using Lipofectamine 3000 Transfection Reagent (Thermo Scientific, USA)
212   according to the manufacturer's instructions. Empty virus vectors were used as negative controls.
213   The primers were 5'-tgttcggaggcttcaactcc-3' (F) and 5'-gacatccaccttcctcgtgt-3' (R). After 72h of
214   transfection, the expression of the green fluorescent protein EGFP in cells was observed under a
215   fluorescence microscope, and stably transfected cells were established by the puromycin (1.5
216   ng/µL) screening method. The rescue experiment was performed based on stably transfected
217   cells.

218   **12. Statistical analysis**
219   The results are expressed as the mean ± standard deviation (SD) from at least three independent
220   experiments. Student's t-test was used to compared the difference between two groups while,
221   one-way analysis of variance (ANOVA) was used to analyze statistical differences between more
222   than two groups. GraphPad Prism software (version 7.04) was used for statistical analysis. A
223   statistically significant difference was defined as $p < 0.05$.

224

225   # Results

226   **1.   Daidzein inhibits the proliferation of 143B and U2OS osteosarcoma cells**
227   Firstly, we explored the effect of daidzein on proliferation of 143B and U2OS osteosarcoma
228   cells. 143B and U2OS cells were treated with gradient concentrations of daidzein (0, 10, 20, 50,
229   100, 200 or 500 µmol/L). After 48 or 72 h treatment, MTT assay was performed to detect the cell
230   proliferation capacity. As shown in Fig.2A-B, daidzein significantly inhibited the proliferation
231   capacity of osteosarcoma cells in a dose- and time-dependent manner. According to the
232   absorbance curve, the 48h 50% inhibiting concentration (IC_{50}) of daidzein on 143B and U2OS
233   cells are 63.59 µmol/L and 125 µmol/L. Meanwhile, we treated normal human hFOB 1.19
234   osteoblasts with the same daidzein dose in 48 and 72 h (Fig. 1C). According to the analysis
235   results of IC_{50} (Fig. 1D), daidzein had a much weaker inhibitory effect on the proliferation of
236   hFOB cells compared with osteosarcoma cells (Student's t-test, $p < 0.05$). Thus, daidzein should
237   be considered relatively safe when applied clinically. Then, we set three concentration treatment
238   groups (143B: 20 µmol/L for the low concentration group, 48h IC_{50} group, and 200 µmol/L for

239 the high concentration group; U2OS: 50 μmol/L for the low concentration group, 48h IC_{50} group,
240 and 200 μmol/L for the high concentration group) for the following experiments. And colony
241 formation assay results also showed that daidzein significantly inhibited the colony formation
242 ability of 143B and U2OS osteosarcoma cells (Fig.2E-F). Thus, daidzein may inhibits the
243 proliferation of 143B and U2OS osteosarcoma cells in a dose- and time-dependent manner.
244 **2. Daidzein induces apoptosis and cell cycle arrest in 143B and U2OS osteosarcoma cells**
245 Hoechst 33342 staining and Annexin V-FITC/PI dual staining detection kits were used to
246 determine the effect of daidzein on apoptosis 143B and U2OS cells. The results indicated that
247 24h of treatment with daidzein (at low, IC_{50}, and high concentrations) considerably increased
248 apoptosis in a dose-dependent manner compared to that of the control group. The results of the
249 flow cytometric analysis showed that the early and late apoptosis rate of daidzein treatment
250 group (at low, IC_{50}, and high concentrations) were significantly lower than that of the control
251 group (Fig.3A-B). Next, we determined whether daidzein was involved in the cell cycle of
252 osteosarcoma cells. According to the cell cycle distribution analyzed by flow cytometry, we
253 found that daidzein increased the percentage of S phase cells but decreased the percentage of
254 G_0/G_1 phase cells in 143B and U2OS cells (Fig.3C-D). These results suggest that daidzein may
255 induce apoptosis and cell cycle arrest in 143B and U2OS osteosarcoma cells.
256 **3. Daidzein suppresses migration ability of and 143B and U2OS osteosarcoma cells**
257 We also explored the influence of daidzein on migration ability of osteosarcoma. 143B and
258 U2OS cells were pretreated with daidzein for 24h before the Transwell assays. Daidzein
259 significantly suppressed cell migration in 143B and U2OS cells, as shown in Fig.3E. Moreover,
260 scratch wound assay revealed that the cell mobility rates in daidzein treatment group were
261 significantly decreased when compared with the control group (Fig.3G). Therefore, daidzein can
262 suppress migration ability of and 143B and U2OS osteosarcoma cells.
263 **4. Daidzein effectively suppresses osteosarcoma growth in xenograft mice model**
264 To investigate the effect of daidzein on osteosarcoma in vivo, an osteosarcoma xenograft mice
265 model was established by subcutaneous implantation of 143B cells in BALB/c nude mice. As
266 shown in Fig.4, the volume and weight of the tumors and tumor growth rate in the daidzein-
267 treated group significantly decreased when compared with those in the control group. H&E
268 staining of the tumor revealed that the number of necrotic cells in the daidzein-treated group was
269 significantly higher than that in the control group (Figure 4E). Furthermore, the body weight of
270 the nude mice was not significantly affected (Figure 4B), indicating that there was little systemic
271 toxicity of daidzein in vivo.
272 **5. Target prediction of daidzein on osteosarcoma through systemic pharmacology analysis**
273 To reveal the mechanism of daidzein regulating biological process of osteosarcoma cells,
274 systemic pharmacology analysis was performed on PharmMapper platform. A total of 243
275 human genes associated with daidzein were predicted by the PharmMapper platform (Table S1).
276 As shown in Figure 5A, a "daidzein-daidzein targets" network was constructed. Osteosarcoma-
277 related genes were collected and combined from DigSeE, DisGeNET, GeneCards, KEGG
278 disease, MalaCards, and Phenopedia (Table S2). After intersecting the two gene sets (Figure 5B),

279 there were 133 common targets of osteosarcoma and daidzein through which daidzein might play
280 a role in regulating the progression of osteosarcoma. After that, 133 target genes associated with
281 daidzein and osteosarcoma were imported into the STRING database for PPI network
282 construction. As shown in Figure 5C and Table S3, there were 133 nodes and 295 interaction
283 edges (interaction score>0.9). To analyze the PPI diagram, the analysis tool in Cytoscape was
284 applied, and the top 30 hub genes were identified and are shown in Figure 5D. Among the top 30
285 hub genes, Src was the node that interacted with the most numerous edges, suggesting that Src
286 may play a vital role of daidzein in regulating biological process of osteosarcoma.
287
288 **6. Src protein may be the target of daidzein**
289 In order to explore whether daidzein can effectively combine with Src and play a regulatory role,
290 we assessed the potential interaction between daidzein and Src through molecular modeling and
291 docking simulation. The 3D structure of daidzein was obtained from the PubChem database
292 (Figure 5E). After adjustment and analysis, the grid size was set to 40×40×40, and we obtained
293 an affinity of -9.1 kcal/mol. As shown in Figure 5F, hydrophobic interactions were formed
294 between daidzein and the following amino acid residues: Ile336, Thr338, Met314, Val323,
295 Phe405, Ala403, Leu393, Asp404, Val281 and Ala293. In brief, these results suggest a strong
296 potential of direct binding between daidzein and Src. Thereafter, we employed GO annotation
297 for the functions of the key target genes. The top 20 highly enriched functional terms are shown
298 in Figure 6A. The key target genes could regulate multiple biological processes, including
299 steroid hormone receptor activity, nuclear receptor activity, ligand-activated transcription factor
300 activity, etc. The KEGG results indicated that these key target genes were involved in multiple
301 signaling pathways, and the top 20 pathways are shown in Figure 6B. Among them, the MAPK
302 signaling pathway was the highest-ranked pathway, with the highest gene ratio as well as the
303 third minimum adjusted P-value (less than $1e^{-07}$). According to previous studies, the MAPK
304 (JNK/ERK/p38) signaling pathway is a downstream molecule of Src kinase (Cui et al. 2017; Gao
305 et al. 2019). Therefore, we further predicted that the Src and MAPK pathways may be involved
306 in the regulation of daidzein on biological process of osteosarcoma.
307
308 **7. Daidzein inhibits phosphorylation of the Src and ERK signaling pathways**
309 **osteosarcoma cells**
310 According to the results of previous systemic pharmacology analysis and molecular docking
311 studies, we detected the protein expression and phosphorylation levels of Src, JNK, ERK and
312 p38 to elucidate the molecular mechanisms by which daidzein affects osteosarcoma cells. As
313 shown in Figure 6C-D, daidzein treatment decreased the expression of p-Src and p-ERK, but the
314 expression levels of Src, JNK, p-JNK, ERK, p38 and p-p38 were not significantly changed.
315 Therefore, we determined that Src and ERK phosphorylation was suppressed in daidzein-treated
316 cells, whereas JNK and p38 phosphorylation was not altered.
317
318 **8. Overexpression of Src rescues inhibitory effect of daidzein on osteosarcoma cells**

319   As shown in Fig.7B-C, overexpression of Src partially restituted the phosphorylation of Src and
320   ERK in osteosarcoma cells treated with daidzein. Moreover, according to MTT assay (Figure
321   7D) and apoptosis analysis by flow cytometry (Figure 7E-F), decreased viability and in
322   osteosarcoma cells treated with daidzein was partially reversed by overexpression of Src.
323   Therefore, it suggests that daidzein may exert anti-osteosarcoma efficiency through the inhibition
324   of the Src kinase-mediated ERK pathway.
325
326   **Discussion**
327   Daidzein is often found in beans such as soybeans, sweet red beans, and kidney beans. Previous
328   studies have shown that it has antioxidative, anti-inflammatory, and anti-aging activities (Ahmad
329   et al. 2016; Choi et al. 2012; Liu et al. 2009; Tomar et al. 2020; Yi et al. 2019; Yu et al. 2020;
330   Živanović et al. 2019). Additionally, daidzein has garnered interest as a natural compound with
331   antitumor effects against a variety of tumors. Several previous studies have investigated the
332   antitumor effects and mechanisms of daidzein. For example, in colon cancer, daidzein induces
333   apoptosis of tumor cells by inhibiting the accumulation of lipid droplets (Liang et al. 2018). In
334   bladder cancer, daidzein exerts antitumor activity via inhibition of the FGFR3 pathway (He et al.
335   2016). Additionally, daidzein has also been shown to enhance the anticancer effect of topotecan
336   and reverse BCRP-mediated drug resistance in breast cancer (Guo et al. 2019), and it inhibits
337   lung metastasis in mice induced by B16F-10 melanoma cells (Menon et al. 1998). In malignant
338   glioma, treatment with subtoxic doses of daidzein in combination with TRAIL induces rapid
339   apoptosis in glioma cells because daidzein overcomes TRAIL resistance by modulating the
340   expression of the intrinsic apoptotic inhibitor bcl-2 (Siegelin et al. 2009).
341   As a kind of nonreceptor protein tyrosine kinase, Src is an important oncogenic biological factor
342   in a variety of malignancies, and the active form of Src is phosphorylated Src (p-Src) (Dehm &
343   Bonham 2004). Src interacts with several protein-tyrosine kinase receptors at the plasma
344   membrane, including EGFR, erbB2, c-Met, PDGFR, IGFR and FGFR. These protein-tyrosine
345   kinase receptors are dysregulated or mutated in a variety of human malignancies, including and
346   not limited to NSCLC, breast cancer, pancreatic cancer, colorectal cancer, bladder cancer,
347   prostate cancer, kidney cancer, ovarian cancer and sarcoma and so on (Roskoski 2015). Src and
348   that of its protein-tyrosine kinase receptors interact with each other. In addition to protein
349   tyrosine kinases, Src-family kinases are also regulated by integrin receptors, G-protein coupled
350   receptors, antigen- and Fc-coupled receptors, cytokine receptors, and steroid hormone receptors
351   (Thomas & Brugge 1997). As the central hub of multiple signaling pathways, Src is involved in
352   the amplification cascade of the intracellular network regulation system, whose downstream
353   pathways include FAK, Akt, Stat3 and MAPK. Src is also involved in the regulation of bone
354   formation and remodeling and may mediate skeletal metastasis of breast, prostate, and lung
355   cancers (Roskoski 2015). Our previous clinical studies have shown that Src/p-Src are potential
356   biomarkers of osteosarcoma, which could promote the progression or metastasis of osteosarcoma
357   and may lead to a poorer prognosis in clinical patients (Hu et al. 2015).

358 In modern civilization, the spectrum of human diseases has changed greatly, from infectious
359 diseases to complex diseases such as tumors, cardiovascular diseases, and diabetes. The
360 occurrence and development of complex diseases often involve multiple genes and signaling
361 pathways in the regulatory network of the organism. Systemic pharmacology aims at biological
362 networks and analyzes the relationship among the drugs, targets and diseases in these networks
363 (Yuan et al. 2017), which is consistent with the treatment concept of complex diseases: to carry
364 out new drug research and drug mechanistic research. The large amount of experimental material
365 and reagents used in previous screening studies has been saved due to the availability of data
366 from the Internet for analysis, thereby greatly saving time and expense.
367

Conclusions

369 In conclusion, through a combination of systemic pharmacology, molecular docking and
370 experimental validation, this study provides powerful proof that daidzein has little negative
371 effect on normal cells and exerts an antitumor effect through the Src-ERK axis, which suggests
372 that daidzein could act as a potential osteosarcoma chemotherapy agent. However, this study has
373 its limitations. First, owing to limitations of time and funds, instead of experimentally validating
374 all target molecules and pathways screened by the network pharmacological analysis, we chose
375 the one with the highest match possibility. Second, we only examined the anti-osteosarcoma
376 effects of daidzein, but we did not validate the mechanism in vivo. In addition, depending on the
377 different cell types and stimuli, MAPKs have a dual role since they can act as activators or
378 inhibitors of apoptosis (Yue & López 2020). Therefore, further indepth study is needed on the
379 specific mechanism by which daidzein inhibits ERK phosphorylation and thus causes apoptosis
380 in osteosarcoma cells. In addition, more basic and clinical studies are needed to establish the role
381 of daidzein in the treatment of osteosarcoma.
382

Acknowledgements

384 The authors thank Dr. Xiaobin Zhu and Bin Ren from the Department of Spine Surgery &
385 Musculoskeletal Tumor, Zhongnan Hospital of Wuhan University, China for assisting in
386 experimental design.

387

References

389 **Ahmad S, Alam K, Hossain MM, Fatima M, Firdaus F, Zafeer MF, Arif Z, Ahmed M, and Nafees**
390   **KA. 2016.** Anti-arthritogenic and cardioprotective action of hesperidin and daidzein in collagen-
391   induced rheumatoid arthritis. *Mol Cell Biochem* 423:115-127. 10.1007/s11010-016-2830-y
392 **Bao C, Namgung H, Lee J, Park HC, Ko J, Moon H, Ko HW, and Lee HJ. 2014.** Daidzein suppresses
393   tumor necrosis factor-α induced migration and invasion by inhibiting hedgehog/Gli1 signaling in
394   human breast cancer cells. *J Agric Food Chem* 62:3759-3767. 10.1021/jf500231t
395 **Berger SI, and Iyengar R. 2009.** Network analyses in systems pharmacology. *Bioinformatics* 25:2466-
396   2472. 10.1093/bioinformatics/btp465
397 **Choi EY, Jin JY, Lee JY, Choi JI, Choi IS, and Kim SJ. 2012.** Anti-inflammatory effects and the
398   underlying mechanisms of action of daidzein in murine macrophages stimulated with Prevotella
399   intermedia lipopolysaccharide. *J Periodontal Res* 47:204-211. 10.1111/j.1600-0765.2011.01422.x

400 **Cui S, Wang J, Wu Q, Qian J, Yang C, and Bo P. 2017.** Genistein inhibits the growth and regulates the
401   migration and invasion abilities of melanoma cells via the FAK/paxillin and MAPK pathways.
402   *Oncotarget* 8:21674-21691. 10.18632/oncotarget.15535
403 **Dehm SM, and Bonham K. 2004.** SRC gene expression in human cancer: the role of transcriptional
404   activation. *Biochem Cell Biol* 82:263-274. 10.1139/o03-077
405 **Gao Z, Zhao GS, Lv Y, Peng D, Tang X, Song H, and Guo QN. 2019.** Anoikis-resistant human
406   osteosarcoma cells display significant angiogenesis by activating the Src kinase-mediated MAPK
407   pathway. *Oncol Rep* 41:235-245. 10.3892/or.2018.6827
408 **Gianferante DM, Mirabello L, and Savage SA. 2017.** Germline and somatic genetics of osteosarcoma -
409   connecting aetiology, biology and therapy. *Nat Rev Endocrinol* 13:480-491.
410   10.1038/nrendo.2017.16
411 **Guo J, Wang Q, Zhang Y, Sun W, Zhang S, Li Y, Wang J, and Bao Y. 2019.** Functional daidzein
412   enhances the anticancer effect of topotecan and reverses BCRP-mediated drug resistance in breast
413   cancer. *Pharmacol Res* 147:104387. 10.1016/j.phrs.2019.104387
414 **Harrison DJ, Geller DS, Gill JD, Lewis VO, and Gorlick R. 2018.** Current and future therapeutic
415   approaches for osteosarcoma. *Expert Rev Anticancer Ther* 18:39-50.
416   10.1080/14737140.2018.1413939
417 **He Y, Wu X, Cao Y, Hou Y, Chen H, Wu L, Lu L, Zhu W, and Gu Y. 2016.** Daidzein exerts anti-
418   tumor activity against bladder cancer cells via inhibition of FGFR3 pathway. *Neoplasma* 63:523-
419   531. 10.4149/neo_2016_405
420 **Hopkins AL. 2008.** Network pharmacology: the next paradigm in drug discovery. *Nat Chem Biol* 4:682-
421   690. 10.1038/nchembio.118
422 **Hu C, Deng Z, Zhang Y, Yan L, Cai L, Lei J, and Xie Y. 2015.** The prognostic significance of Src and
423   p-Src expression in patients with osteosarcoma. *Med Sci Monit* 21:638-645.
424   10.12659/msm.892803
425 **Jin S, Zhang QY, Kang XM, Wang JX, and Zhao WH. 2010.** Daidzein induces MCF-7 breast cancer
426   cell apoptosis via the mitochondrial pathway. *Ann Oncol* 21:263-268. 10.1093/annonc/mdp499
427 **Khanna C, Fan TM, Gorlick R, Helman LJ, Kleinerman ES, Adamson PC, Houghton PJ, Tap WD,
428   Welch DR, Steeg PS, Merlino G, Sorensen PH, Meltzer P, Kirsch DG, Janeway KA, Weigel
429   B, Randall L, Withrow SJ, Paoloni M, Kaplan R, Teicher BA, Seibel NL, Smith M, Uren A,
430   Patel SR, Trent J, Savage SA, Mirabello L, Reinke D, Barkaukas DA, Krailo M, and
431   Bernstein M. 2014.** Toward a drug development path that targets metastatic progression in
432   osteosarcoma. *Clin Cancer Res* 20:4200-4209. 10.1158/1078-0432.ccr-13-2574
433 **Kleinerman E. 2016.** Maximum benefit of chemotherapy for osteosarcoma achieved-what are the next
434   steps? *Lancet Oncol* 17:1340-1342. 10.1016/s1470-2045(16)30270-4
435 **Li Z, Li X, Xu D, Chen X, Li S, Zhang L, Chan MTV, and Wu WKK. 2020.** An update on the roles of
436   circular RNAs in osteosarcoma. *Cell Prolif*:e12936. 10.1111/cpr.12936
437 **Lian Z, Niwa K, Tagami K, Hashimoto M, Gao J, Yokoyama Y, Mori H, and Tamaya T. 2001.**
438   Preventive effects of isoflavones, genistein and daidzein, on estradiol-17beta-related endometrial
439   carcinogenesis in mice. *Jpn J Cancer Res* 92:726-734. 10.1111/j.1349-7006.2001.tb01154.x
440 **Liang YS, Qi WT, Guo W, Wang CL, Hu ZB, and Li AK. 2018.** Genistein and daidzein induce
441   apoptosis of colon cancer cells by inhibiting the accumulation of lipid droplets. *Food & nutrition
442   research* 62. 10.29219/fnr.v62.1384
443 **Liu MH, Lin YS, Sheu SY, and Sun JS. 2009.** Anti-inflammatory effects of daidzein on primary
444   astroglial cell culture. *Nutr Neurosci* 12:123-134. 10.1179/147683009x423274
445 **Lo FH, Mak NK, and Leung KN. 2007.** Studies on the anti-tumor activities of the soy isoflavone
446   daidzein on murine neuroblastoma cells. *Biomed Pharmacother* 61:591-595.
447   10.1016/j.biopha.2007.08.021
448 **Luu AK, and Viloria-Petit AM. 2020.** Targeting Mechanotransduction in Osteosarcoma: A
449   Comparative Oncology Perspective. *Int J Mol Sci* 21. 10.3390/ijms21207595

450 **Magee PJ, Allsopp P, Samaletdin A, and Rowland IR. 2014.** Daidzein, R-(+)equol and S-(-)equol
451   inhibit the invasion of MDA-MB-231 breast cancer cells potentially via the down-regulation of
452   matrix metalloproteinase-2. *Eur J Nutr* 53:345-350. 10.1007/s00394-013-0520-z
453 **Menon LG, Kuttan R, Nair MG, Chang YC, and Kuttan G. 1998.** Effect of isoflavones genistein and
454   daidzein in the inhibition of lung metastasis in mice induced by B16F-10 melanoma cells. *Nutr*
455   *Cancer* 30:74-77. 10.1080/01635589809514644
456 **Roskoski R, Jr. 2015.** Src protein-tyrosine kinase structure, mechanism, and small molecule inhibitors.
457   *Pharmacol Res* 94:9-25. 10.1016/j.phrs.2015.01.003
458 **Salvatori L, Caporuscio F, Coroniti G, Starace G, Frati L, Russo MA, and Petrangeli E. 2009.**
459   Down-regulation of epidermal growth factor receptor induced by estrogens and phytoestrogens
460   promotes the differentiation of U2OS human osteosarcoma cells. *J Cell Physiol* 220:35-44.
461   10.1002/jcp.21724
462 **Siegelin MD, Gaiser T, Habel A, and Siegelin Y. 2009.** Daidzein overcomes TRAIL-resistance in
463   malignant glioma cells by modulating the expression of the intrinsic apoptotic inhibitor, bcl-2.
464   *Neurosci Lett* 454:223-228. 10.1016/j.neulet.2009.03.031
465 **Singh-Gupta V, Zhang H, Yunker CK, Ahmad Z, Zwier D, Sarkar FH, and Hillman GG. 2010.**
466   Daidzein effect on hormone refractory prostate cancer in vitro and in vivo compared to genistein
467   and soy extract: potentiation of radiotherapy. *Pharm Res* 27:1115-1127. 10.1007/s11095-010-
468   0107-9
469 **Thomas SM, and Brugge JS. 1997.** Cellular functions regulated by Src family kinases. *Annu Rev Cell*
470   *Dev Biol* 13:513-609. 10.1146/annurev.cellbio.13.1.513
471 **Thomford NE, Senthebane DA, Rowe A, Munro D, Seele P, Maroyi A, and Dzobo K. 2018.** Natural
472   Products for Drug Discovery in the 21st Century: Innovations for Novel Drug Discovery. *Int J*
473   *Mol Sci* 19. 10.3390/ijms19061578
474 **Tomar A, Kaushik S, Khan SI, Bisht K, Nag TC, Arya DS, and Bhatia J. 2020.** The dietary
475   isoflavone daidzein mitigates oxidative stress, apoptosis, and inflammation in CDDP-induced
476   kidney injury in rats: Impact of the MAPK signaling pathway. *J Biochem Mol Toxicol* 34:e22431.
477   10.1002/jbt.22431
478 **Wang HZ, Zhang Y, Xie LP, Yu XY, and Zhang RQ. 2002.** Effects of genistein and daidzein on the
479   cell growth, cell cycle, and differentiation of human and murine melanoma cells(1). *J Nutr*
480   *Biochem* 13:421-426. 10.1016/s0955-2863(02)00184-5
481 **Yi Y, Adrjan B, Li J, Hu B, and Roszak S. 2019.** NMR studies of daidzein and puerarin: active anti-
482   oxidants in traditional Chinese medicine. *J Mol Model* 25:202. 10.1007/s00894-019-4090-8
483 **Yu L, Blackburn GL, and Zhou JR. 2003.** Genistein and daidzein downregulate prostate androgen-
484   regulated transcript-1 (PART-1) gene expression induced by dihydrotestosterone in human
485   prostate LNCaP cancer cells. *J Nutr* 133:389-392. 10.1093/jn/133.2.389
486 **Yu Z, Yang L, Deng S, and Liang M. 2020.** Daidzein ameliorates LPS-induced hepatocyte injury by
487   inhibiting inflammation and oxidative stress. *Eur J Pharmacol* 885:173399.
488   10.1016/j.ejphar.2020.173399
489 **Yuan H, Ma Q, Cui H, Liu G, Zhao X, Li W, and Piao G. 2017.** How Can Synergism of Traditional
490   Medicines Benefit from Network Pharmacology? *Molecules* 22. 10.3390/molecules22071135
491 **Yue J, and López JM. 2020.** Understanding MAPK Signaling Pathways in Apoptosis. *Int J Mol Sci* 21.
492   10.3390/ijms21072346
493 **Zhang Q, Xie H, Chen D, Yu B, Huang Z, Zheng P, Mao X, Yu J, Luo Y, Luo J, and He J. 2018.**
494   Dietary Daidzein Supplementation During Pregnancy Facilitates Fetal Growth in Rats. *Mol Nutr*
495   *Food Res* 62:e1800921. 10.1002/mnfr.201800921
496 **Zheng W, Sun R, Yang L, Zeng X, Xue Y, and An R. 2017.** Daidzein inhibits choriocarcinoma
497   proliferation by arresting cell cycle at G1 phase through suppressing ERK pathway in vitro and in
498   vivo. *Oncol Rep* 38:2518-2524. 10.3892/or.2017.5928

499 **Živanović J, Jarić I, Ajdžanović V, Mojić M, Miler M, Šošić-Jurjević B, Milošević V, and Filipović**
500 **B. 2019.** Daidzein upregulates anti-aging protein Klotho and NaPi 2a cotransporter in a rat model
501 of the andropause. *Ann Anat* 221:27-37. 10.1016/j.aanat.2018.08.001
502

Figure 1

The methodological flowchart of this study.

This study firstly experimentally demonstrated the therapeutic effect of daidzein on osteosarcoma, then through the exploration of network pharmacology and molecular docking technology, key molecules and pathways were targeted and experimentally validated. Website links: DigSeE (http://210.107.182.61/geneSearch/) DisGeNET (http://www.disgenet.org/), GeneCards (https://www.genecards.org/) KEGG disease (https://www.kegg.jp/kegg/disease/) MalaCards (http://www.malacards.org/) Phenopedia (https://phgkb.cdc.gov/PHGKB/startPagePhenoPedia.action) PubChem (https://pubchem.ncbi.nlm.nih.gov/) PharmMapper (http://www.lilabecust.cn/pharmmapper/) VENNY 2.1.0 (https://bioinfogp.cnb.csic.es/tools/venny/).
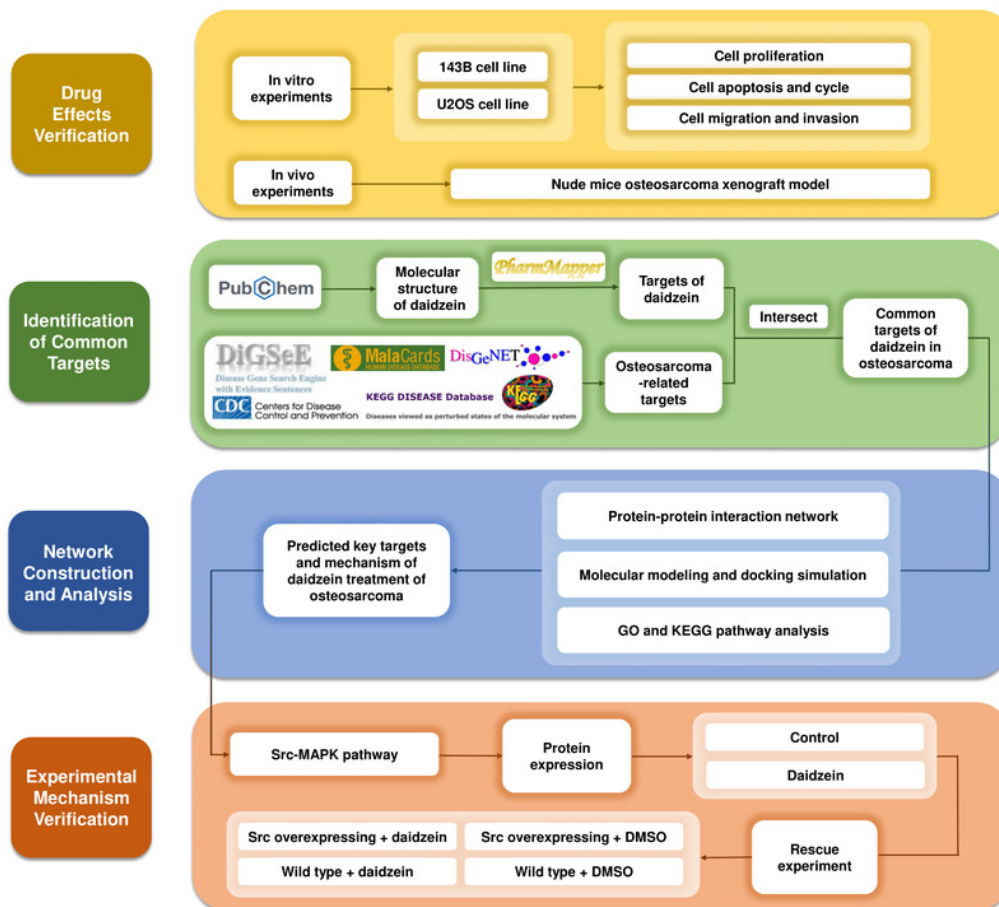
Figure 2

Daidzein inhibited cell proliferation and induced apoptosis in vitro.

(A) MTT analysis of 143B and U2OS cells treated with different concentrations of daidzein for 48 or 72 h. MTT assay was performed in sextuplicate. Dose- and time-dependent inhibition of cell growth could be observed ($P < 0.0001$, ANOVA analysis). (B) IC_{50} values in 143B and U2OS cells after 48 or 72 h of daidzein treatment. (C) MTT analysis of hFOB cells treated with different concentrations of daidzein for 48 or 72 h. (D) IC_{50} values in non-tumor cells hFOB after 48 or 72 h of daidzein treatment. (E) Seven-day colony formation assay of 143B and U2OS cells treated with different concentrations of daidzein. (F) Colony counts in 143B and U2OS cells treated with different concentrations of daidzein from four independent experiments. (G) Hoechst 33342 staining assay of 143B and U2OS cells treated with different concentrations of daidzein. (Solid bars and errors represent the mean ± SEM. Individual values were shown as dots of different shapes. Student's t-test, $^{*}p < 0.05$, $^{**}p < 0.01$, $^{***}p <0.001$, $^{****}p <0.0001$ versus control group.)
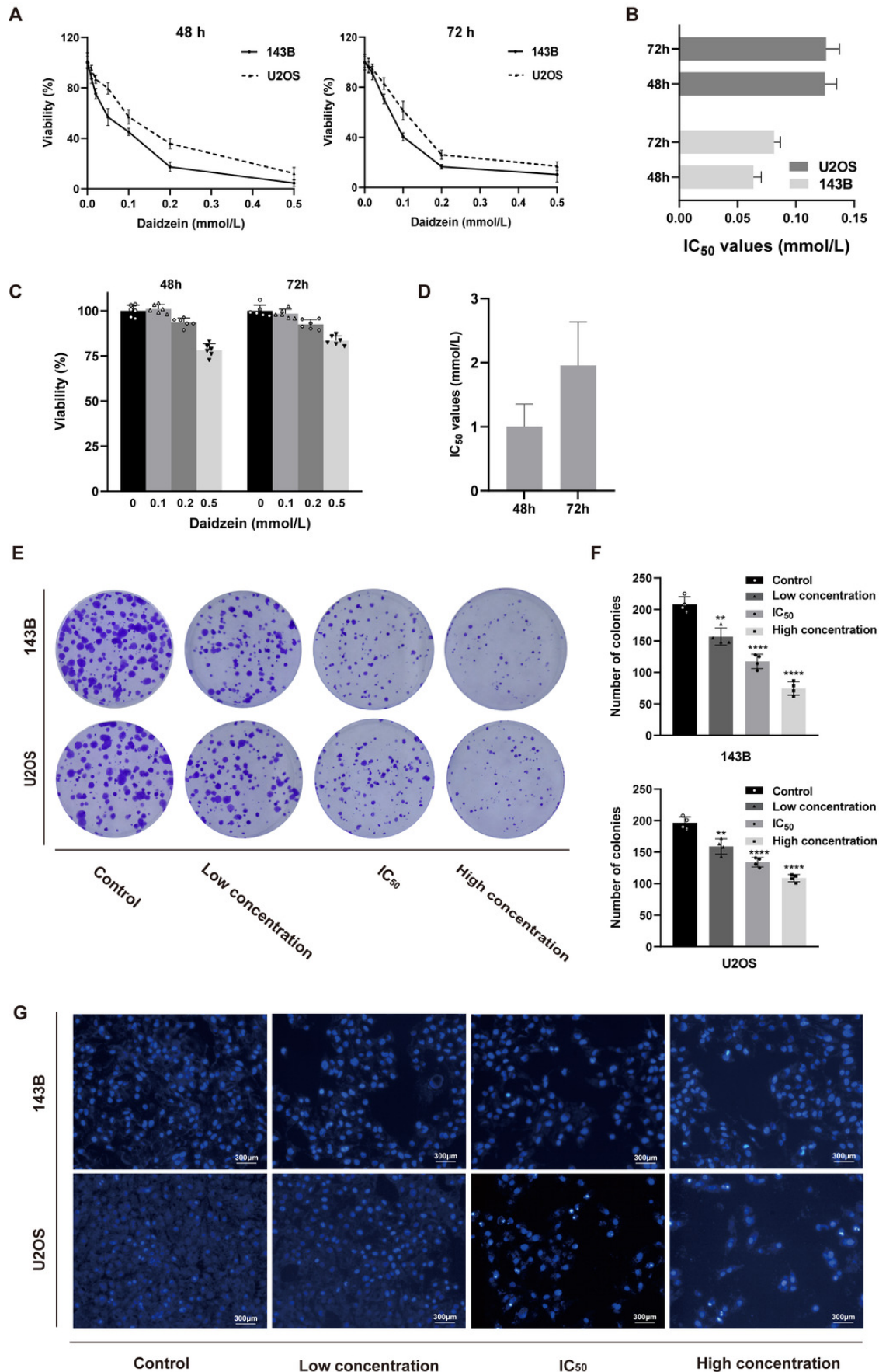
Figure 3

Incubation of osteosarcoma cells with daidzein promoted apoptosis and cell cycle arrest when inhibited migration.

(A) 143B and U2OS cells treated with different concentrations of daidzein were stained with Annexin V-FITC/PI, analyzed by flow cytometry. Quantitative analysis of apoptotic cells from three independent experiments. (B) Cell cycle detection of 143B and U2OS cells treated with different concentrations of daidzein, examined by flow cytometry. (C) Quantitative analysis of cycle distribution from three independent experiments. (D) Transwell assay of 143B and U2OS cells pretreated with different concentrations of daidzein. F) Invaded cell counts in 143B and U2OS cells pretreated with different concentrations of daidzein. (E) Scratch wound migration analysis of osteosarcoma cells treated with different concentrations of daidzein. (F) Wound closure rates in osteosarcoma cells treated with different concentrations of daidzein. (Solid bars and errors represent the mean ± SEM, Individual values were shown as dots of different shapes, Student's t-test, $^{*}p < 0.05$, $^{**}p < 0.01$, $^{***}p < 0.001$, $^{****}p < 0.0001$ versus control group.)
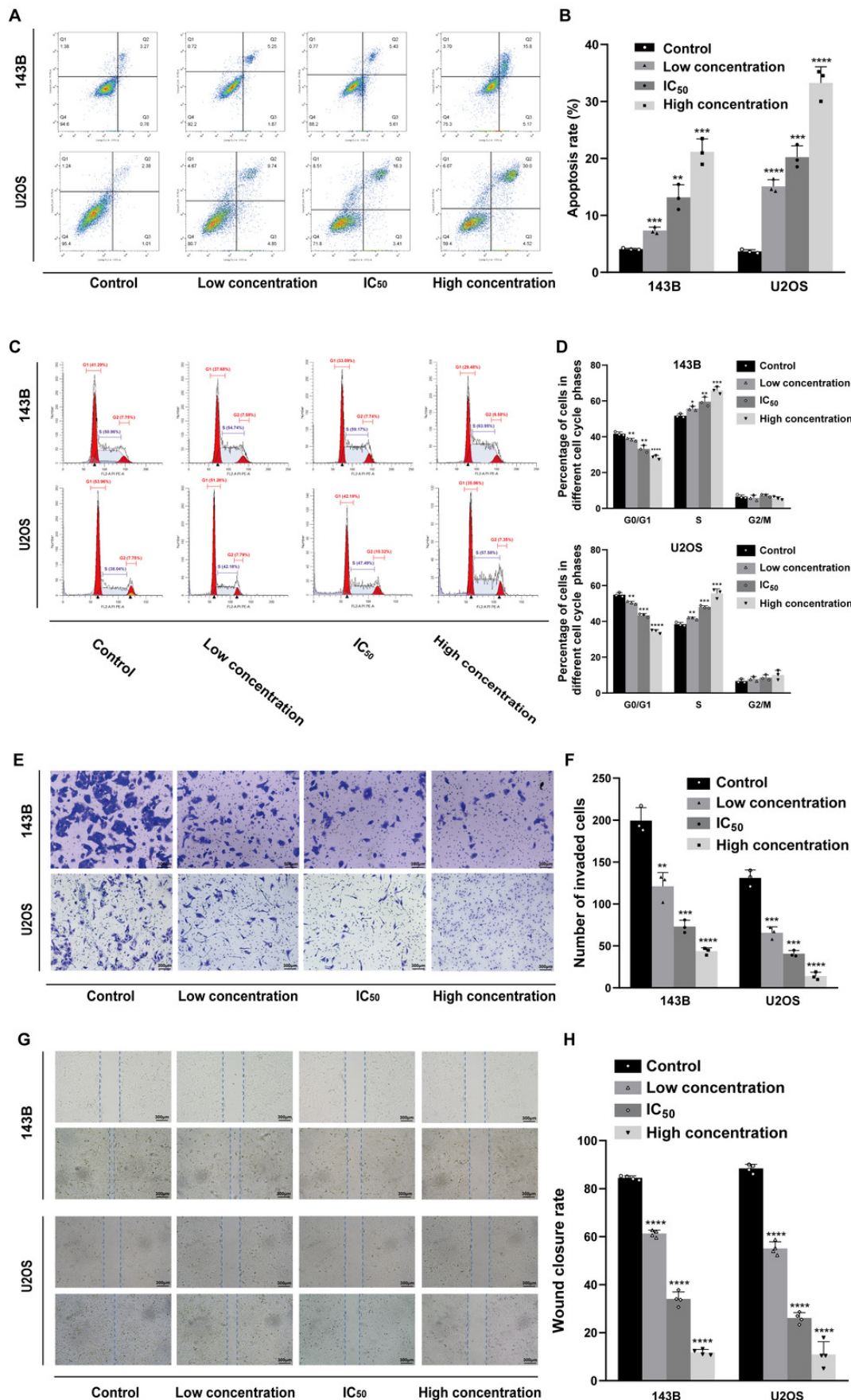
Figure 4

Daidzein exerts antitumor effects in vivo without obvious toxicity.

(A) Gross observation of osteosarcoma xenograft mice on the day the mice were sacrificed. (B) Body weight during the daidzein injection. There was no significant difference between the two groups. (ANOVA analysis) (C) Gross observation of tumor tissue on the day the mice were sacrificed. (D) Tumor volume during the daidzein injection. Time-dependent inhibition of cell growth could be observed ($P < 0.0001$, ANOVA analysis) (E) H&E staining of the tumor. The daidzein group showed obvious tumor necrosis. (F) Tumor weight on day 16. Solid bars and errors represent the mean ± SEM, Student's t-test, ****$p <0.0001$ versus control group.
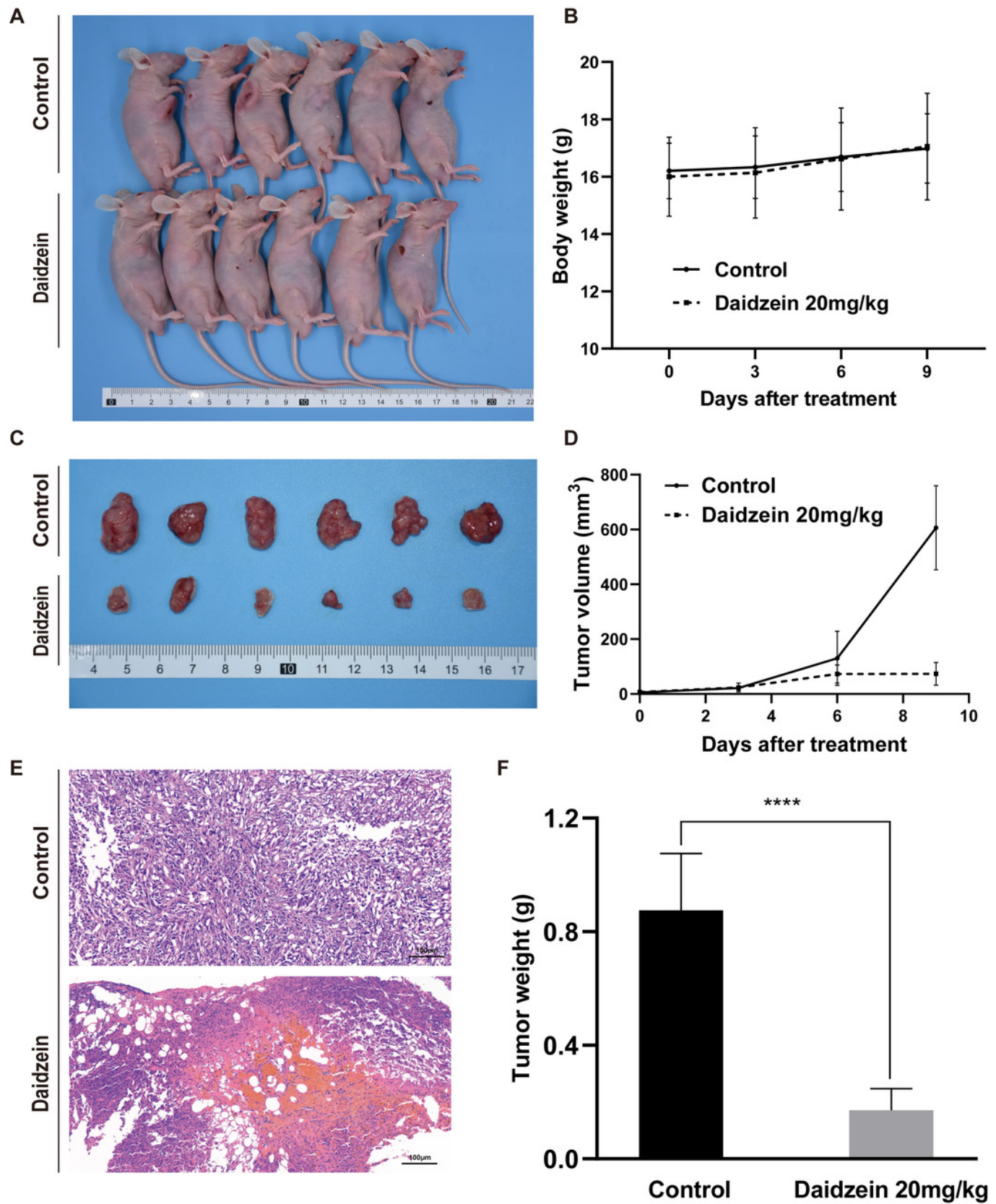
Figure 5

Src is the most likely target molecule for direct binding by daidzein.

(A) Network of daidzein-target genes. Purple diamonds represent daidzein; green circles represent target genes of daidzein. (B) Venn diagram revealing the common target genes of daidzein against osteosarcoma. (C) Protein-protein interaction (PPI) network. Nodes: common targets of daidzein and osteosarcoma; Edges: PPIs between targets of daidzein and their interaction partners. (D) The top 30 hub genes in the PPI network that interacted with the most numerous edges. (E) The Ball and Stick 3D structure of daidzein. The gray ball represents the carbon atom when the red ball represents the oxygen atom, and the small white ball represents the hydrogen atom. (F) Molecular docking simulation predicted the amino acid residues bound by daidzein. (G) Molecular docking simulation of daidzein to Src protein. Sticks represent the three-dimensional structure of daidzein; the surface represents the protein structure of Src protein.
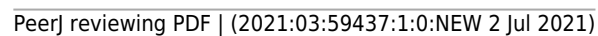
Figure 6

Daidzein inhibits phosphorylation of Src and ERK in osteosarcoma cells.

(A) The top 20 highly enriched functional terms analyzed by GO enrichment. (B) The top 20 highly enriched signaling pathways analyzed by KEGG enrichment. (C) Western blot results of the Src-MAPK pathway in 143B and U2OS cells treated with different concentrations of daidzein. (D) Quantitative analysis of western blot. Solid bars and errors represent the mean ± SEM, Individual values were shown as dots of different shapes. Student's t-test, $^*p < 0.05$, $^{**}p < 0.01$ versus control group.
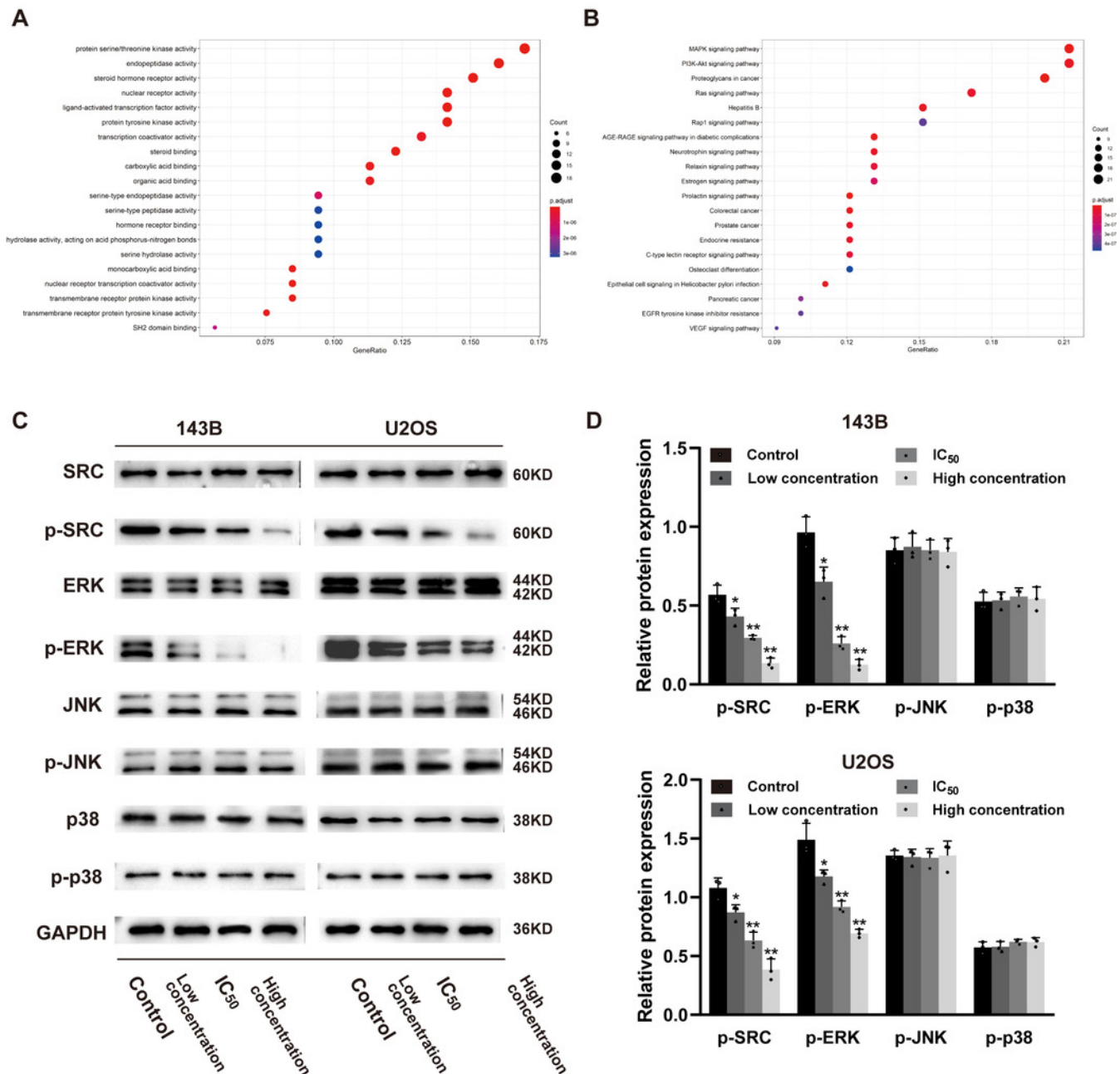
Figure 7

Daidzein exerts antitumor effects through the Src-ERK pathway in osteosarcoma confirmed by the Src overexpression rescue experiments.

(A) The expression of the green fluorescent protein EGFP in Src-overexpressing 143B and U2OS cells was observed under a fluorescence microscope. (B) Western blot results of the Src-ERK pathway in the Src overexpression rescue experiments. (C) Quantitative analysis of western blot of the Src overexpression rescue experiments. (D) MTT analysis of the Src overexpression rescue experiments. (E) Apoptotic cells were detected by the V-FITC/PI double staining assay in the Src overexpression rescue experiments. (F) Quantitative analysis of apoptotic cells from three independent experiments. (Solid bars and errors represent the mean ± SEM, Individual values were shown as dots of different shapes. Student's t-test, $^{*}p < 0.05$, $^{**}p < 0.01$, $^{***}p <0.001$ versus control group.)